Analyst

Cite this: *Analyst*, 2012, **137**, 3004

www.rsc.org/analyst

PAPER

Examining changes in cellular communication in neuroendocrine cells after noble metal nanoparticle exposure†

Sara A. Love, Zhen Liu and Christy L. Haynes*

Received 8th January 2012, Accepted 8th February 2012
DOI: 10.1039/c2an00034b

As nanoparticles enjoy increasingly widespread use in commercial applications, the potential for unintentional exposure has become much more likely during any given day. Researchers in the field of nanotoxicity are working to determine the physicochemical nanoparticle properties that lead to toxicity in an effort to establish safe design rules. This work explores the effects of noble metal nanoparticle exposure in murine chromaffin cells, focusing on examining the effects of size and surface functionality (coating) in silver and gold, respectively. Carbon-fibre microelectrode amperometry was utilized to examine the effect of exposure on exocytosis function, at the single cell level, and provided new insights into the compromised functions of cells. Silver nanoparticles of varied size, between 15 and 60 nm diameter, were exposed to cells and found to alter the release kinetics of exocytosis for those cells exposed to the smallest examined size. Effects of gold were examined after modification with two commonly used 'bio-friendly' polymers, either heparin or poly (ethylene glycol), and gold nanoparticles were found to induce altered cellular adhesion or the number of chemical messenger molecules released, respectively. These results support the body of work suggesting that noble metal nanoparticles perturb exocytosis, typically altering the number of molecules and kinetics of release, and supports a direct disruption of the vesicle matrix by the nanoparticle. Overall, it is clear that various nanoparticle physicochemical properties, including size and surface coating, do modulate changes in cellular communication *via* exocytosis.

Introduction

According to the Project on Emerging Nanotechnologies, as of March 2011, the number of consumer products containing nanomaterials has grown over 500% since 2005.[1] This increase in daily-use nanoparticle-containing products, from beer bottles to bedding, is due to the novel chemical and physical properties that give consumer goods improved characteristics, such as enhanced gas permeability, transparency, or stain resistance. However, this also means that there is significantly more potential for accidental nanoparticle exposure throughout any given day. As the potential of accidental exposure to nanomaterials continues to grow, researchers in the field of nanoparticle toxicity are attempting to understand what the risk of such exposure is, determine a method to predict potential nanoparticle toxicity, and address the concerns of regulators and the public regarding nanoparticles. A goal of the nanoparticle toxicity field is to determine the nanoparticle physicochemical properties that are key factors in their toxicity, in hopes of generating a predictive system that will facilitate safe nanoparticle design. Well-characterized nanoparticles and systematic evaluation of nanoparticle toxicity will provide the knowledge necessary to build this predictive system.

There are many classes of nanomaterials; of these, noble metal nanomaterials provide a particularly relevant platform to systematically examine physicochemical parameters important to nanotoxicity. Noble metal nanomaterials are widely used commercially (compared to other nanoscale materials),[1] easy to synthesize, and display a variety of physicochemical characteristics that are readily tailored for systematic study. Two such characteristics, which may be key factors in nanoparticle toxicity, are size and surface functionality (coating). As covered in a recent review article,[2] nanoparticle size can have many impacts relating to toxicity such as tissue distribution, protein adsorption, or rate of uptake. Differences in size could also alter the mechanism of nanoparticle uptake and have downstream effects on toxicity due to differences in nanoparticle localization and corresponding microenvironments within the cell. In the case of surface functionalization, studies have shown that subtle changes in surface chemistry lead to different adsorbed protein profiles on the surface of nanoparticles once exposed to complex biological media.[3–5] A common modification to modulate this interaction is the use of a bio-friendly polymer surface coating; one commonly used polymer is poly(ethylene glycol) (PEG).[6,7] Both Ag and Au

207 Pleasant Street SE, Smith & Kolthoff Halls, Minneapolis, Minnesota, USA. E-mail: chaynes@umn.edu; Fax: +612 626 7541; Tel: +612 626 1096

† This article is part of a themed issue highlighting the targeted study of single units, such as molecules, cells, organelles and pores – The "Single" Issue, guest edited by Henry White.

nanoparticles are widely used for their generally considered known toxicity or lack thereof, respectively. Numerous studies have examined both Ag and Au nanoparticle toxicity, with a variety of nanoparticle synthesis methods, shapes, doses and assays.[8–11] While these and other studies have examined the toxicity of various noble metal nanomaterials, consensus is currently lacking on the key physicochemical properties and the mechanisms of noble metal nanoparticle toxicity. Because both nanoparticle size and surface chemistry likely influence how cells interact with nanoparticles, these two parameters are the focus of this work. Some recent single cell studies, with carbon-fibre microelectrode amperometry (CFMA), have examined a variety of both Au and Ag nanoparticles, though none of these examine the effect of nanoparticle size or polymeric surface modifications.[12–14] These studies have found that, while these nanoparticles do not necessarily alter cellular viability, they can alter the secretion of signaling molecules during cellular communication. The hypothesis of this work is that both nanoparticle size and polymeric surface coatings will modulate this disruption of cellular function.

Herein, this study extends previous work[12] exploring the effects of nanoparticles on murine adrenal medullary chromaffin (MAMC) cells by considering a size series (between 15 and 60 nm diameter) of citrate-capped Ag nanoparticles and 2 surface-modified Au nanoparticles. The two surface modifications were chosen to examine 'bio-friendly' polymers, specifically poly-(ethylene glycol) or heparin, as previous work[12–14] suggests a direct interaction between the nanoparticle and the vesicles' biopolymer matrix. As seen with other Ag and Au nanoparticles, the data collected herein reveals that nanoparticle exposure does not alter the viability of the examined cells but does alter cellular communication release parameters. Size was found to impact exocytosis for the smallest studied Ag nanoparticle, while differences in surface coating for Au nanoparticles were found to disrupt cellular communication (pegylated Au) and adhesion (heparinized Au).

Experimental

Chemicals & reagents

All chemicals were obtained from Sigma Aldrich except the cell culture materials, which were obtained from Invitrogen; all were used without further purification. A Millipore Milli-Q system (Billerica, MA) generated all H_2O used.

Nanoparticle synthesis & characterization

Prior to nanoparticle synthesis, all glassware was washed in aqua regia (3 : 1 HCl:HNO_3), rinsed, and dried. After synthesis, all nanoparticles were purified (*via* centrifugation or dialysis for 3 days), resuspended in H_2O, and then characterized.

A series of Ag nanoparticles, between roughly 15 and 60 nm diameter, were synthesized following a previously described method.[15] In short, sodium borohydride reduced citrate-capped Ag (seed) nanoparticles were grown to larger sizes by boiling seed nanoparticles with additional sodium citrate and differing amounts of silver nitrate. To remove any remaining soluble precursors, all nanoparticles were centrifuged, resuspended (in H_2O), and dialyzed for three days. All nanoparticles were characterized after this cleanup procedure.

Gold nanoparticle synthesis followed previously published reports to yield pegylated Au (Au PEG).[16,17] Briefly, for Au PEG nanoparticles, seed nanoparticles were synthesized using a standard citrate reduction. These citrate-capped precursor nanoparticles were then allowed to stir overnight with thiolated poly(ethylene glycol) (PEG, MW = 5000) to allow surface ligand exchange. A second Au preparation, using a previously published procedure,[18] was used to produce heparin-capped Au nanoparticles (Au HEP). Briefly, hydrogen tetrachloroaurate was reduced by heparin in a one-pot synthesis. As is typical for gold colloid synthesis, as the solution was boiled for one hour, the solution turned from clear to a reddish-purple color, indicating the formation of colloidal nanoparticles.

Nanoparticle characterization included examination of the nanoparticle localized surface plasmon resonance (LSPR) with UV-vis spectroscopy (Ocean optics USB 2000, Dunedin, FL) and the ζ-potential (ZetaPALS, Brookhaven Instruments, Holtsville, NY). Size analysis was performed *via* dynamic light scattering (DLS, on the ZetaPALS instrument) and by transmission electron microscopy (TEM) using a JEOL 1200EX (Tokyo, Japan) with a 120 kV accelerating voltage, where a minimum of 190 nanoparticles were measured to establish size.

Cell culture

As with related previous work,[12] the model cell of study was the MAMC cell due to its well-known exocytosis parameters.[19] All MAMCs were harvested from wild-type brown male mice (C57BL/6J, Jackson Laboratories, Bar Harbor, ME), in accordance with University of Minnesota Institutional Animal Care and Use Committee practices (approved protocol #0509A75006). For bulk studies, including viability, ICP-AES, and TEM uptake preparations, the University of Minnesota tissue-sharing program provided mice (of a mixed genetic background) for MAMC procurement. In all cases, mice were euthanized, the adrenal glands were removed and transported in cold Dulbecco's modified eagle medium with Ham's nutrient 12 mix (DMEM/F-12) media. All glands were dissected to isolate the cells of the medullary region; this was done in chilled Locke's buffer, composed of 154 mM sodium chloride, 3.6 mM potassium chloride, 5.6 mM sodium bicarbonate, 5.6 mM glucose, and 10 mM HEPES in sterile water, pH adjusted to 7.2. Once the medulla region was isolated, the tissue was digested in neutral protease (Worthington Enzyme, Lakewood, NJ) for 30 min (25 U mL^{-1} at 37 °C), washed with PBS, and triturated in DMEM/F-12 media to obtain suspended single cells. Suspended cells were cultured in 35 mm petri dishes or multi-well plates, maintained in a 5% CO_2 atmosphere at 37 °C until use and throughout experimental exposure.

Viability & nanoparticle uptake

All bulk cell suspensions were plated into multi-well plates at a density of 1×10^5 cells mL^{-1}; cells were incubated for 1 h, to ensure adherence, allow cells to recover from harvesting and return to normal function before beginning nanoparticle exposure. Each condition included cell exposure to either phosphate buffered saline (PBS) or one type of nanoparticle for 24 h in at least three replicate wells. For the Ag size series, the final

nanoparticle exposure concentration is represented as a nM (nanoparticle), similar to previous work with heterogeneous Ag nanoparticles (at 1 nM).[12] The nanoparticle concentration for the two Au nanoparticle types examined was at a final concentration of 10 μg mL^{-1}; this dose was selected to facilitate comparison with other recent work with surface-modified Au.[14] At the end of nanoparticle exposure, cells were washed with PBS, and then either viability or uptake was assessed.

Cells were examined for viability with the commonly used MTT assay. Briefly, cells were exposed to 3-[4,5-dimethylthiazol-2-yl]-2,5-diphenyltetrazolium bromide (MTT) in serum-free DMEM/F-12 media for 2 h, allowing the cells with active mitochondria to convert the MTT compound into an insoluble formazan dye. The multi-well plate was centrifuged for 5 min at 150xg, and then the MTT-containing media was removed and replaced with DMSO to dissolve any formazan crystals. The dissolved formazan was then moved to a new 96 well plate, where absorbance (at 570 nm) was read with a microplate reader (Biotek, Winooski, VT), and viability was calculated as a percentage of the negative (PBS exposed) control.

For studies of nanoparticle uptake by cells, both ICP-AES and TEM were performed to quantify uptake and examine localization within the cell, respectively. ICP-AES preparation was performed as previously described.[12] The preparation was performed upon completion of nanoparticle exposure, in brief, by cell lysis with concentrated acid and sonication of the solution for at least 30 min. Standard solutions were used for calibration for either Au or Ag (as appropriate); yttrium was used as an internal standard. All samples were analyzed with a Perkin Elmer Optima 3000DV ICP-AES system (Waltham, MA) for Au (emission at 242.795 nm) or Ag (emission at 328.068 nm). TEM preparation was performed as described previously.[12] Briefly, cells were fixed with gluteraldehyde, dehydrated with alcohol, stained with osmium and embedded in Epon resin. Once embedded, the samples (in resin) were dried and thin sectioned (~200 nm), stained with uranyl acetate and lead citrate, and imaged (60 kV accelerating voltage).

Carbon-fibre microelectrode amperometry

Microelectrode fabrication was done using previously published methods.[14,20] In brief, a single carbon fibre was inserted into a glass capillary, pulled, trimmed, epoxied, cured and beveled (45° angle). On the day of CFMA experiments, electrodes were polished and allowed to soak in activated carbon-saturated isopropyl alcohol. Stimulating pipettes, empty glass capillaries, were pulled as described previously.[12]

As with bulk assays, cell media with nanoparticles was removed at the end of the 24 h exposure period, cells were washed and maintained in Tris buffer (composed of 300 mM sodium chloride, 12.5 mM trishydroxymethylaminomethane, 8.4 mM potassium chloride, 5.6 mM α-D-glucose, 4.5 mM calcium chloride, and 4.2 mM magnesium chloride) during CFMA measurements. CFMA measurements were performed as described previously,[11–13] where cells were examined on an inverted microscope (Nikon TE200U, Melville, NY) equipped with a single channel temperature controller (TC-324B, Warner Instruments, Hamden, CT) and Burleigh PCS500 micromanipulators (Olympus, Center Valley, PA).

As previously described, once the petri dish buffer temperature equilibrated at 37 °C, cellular exocytosis release was probed following a single stimulation (composed of 60 mM K^+ in Tris buffer, 3 s into data recording) introduced approximately 50 μm from the cell surface. Microelectrodes were positioned at the surface of the cell and held at a potential capable of oxidizing epinephrine/norepinephrine (+700 mV *versus* Ag/AgCl) released from cells for 30 s. Traces were collected from cells within two hours of removal of plates from the incubator, yielding between 5 and 25 traces per condition per experiment. Data was collected as previously described,[12–14] using an Axopatch™ 200B potentiostat (Molecular Devices, Inc., Sunnyvale, CA) with low-pass bessel filtering (5 kHz), amplified (20 mV pA^{-1}), and collected with a breakout box (fabricated in house). The breakout box was controlled by Tarheel Electrochemistry module (Chapel Hill, NC) run in LabVIEW™ (National Instruments, Austin, TX), and collected data was digitally filtered at 500 Hz before spike analysis in MiniAnalysis software (Synaptosoft, Fort Lee, NJ). Spikes were selected, excluding spikes not meeting the threshold of 5 times the RMS current noise with a spike area greater than 60 fC, and individual spike parameters were analyzed. Spike parameters were averaged for each experimental condition; data was pooled across multiple days when control conditions were found to be statistically indistinguishable ($p > 0.05$ by student's t-test). Pooled spike parameters that were found to be outside of 2 times the log standard deviation for the log average for a given condition, as previously described,[12] were excluded. Spike parameters from each experimental condition were assessed for significant differences from the control in Graphpad Prism (La Jolla, CA) using ANOVA ($p < 0.05$) with the Dunnett's post test ($p < 0.05$) to compare between the control and experimental conditions, and are reported as mean ± standard error of the mean (SEM).

Interpretation of spike parameters can provide insight into a variety of exocytosis aspects, including quantal release for vesicles (Q) and the kinetics of vesicle release ($T_{1/2}$). Integration of the current for each individual spike yields the spike-associated charge, which can be converted to the number of molecules of epinephrine/norepinephrine released from vesicles by using the Faraday equation for a two electron process. Quantal release can inform our understanding of the loading and storage of epinephrine/norepinephrine in the vesicles and possible perturbations of that storage by nanoparticle uptake/localization within vesicles.[12–14] The spike full-width at half-maximum ($T_{1/2}$) parameter provides information about the kinetics of release from the vesicle and possible changes in the driving forces responsible for expulsion of the contents of the vesicle.

Results & discussion

In an attempt to improve upon the current understanding of noble metal nanoparticle toxicity, a systematic study of the exposure effects on exocytosis was undertaken to vary two separate noble metal nanoparticle physicochemical properties. To examine the effect of size on nanoparticle alterations in exocytosis, a series of spherical Ag nanoparticles were synthesized. As the maximal range of nanoparticle uptake has been found to be between 10 and 70 nm diameter for Au nanoparticles,[21] here we examine three Ag nanoparticles within that

range. The average diameters were assessed by TEM and were measured to be 18.6 ± 5.1 (Ag A), 36.0 ± 6.1 (Ag B), and 54.5 ± 7.8 (Ag C) nm, shown in Fig. 1A, based on measurements from at least 190 imaged nanoparticles. All three Ag nanoparticles were found to have negative ζ-potentials, of magnitudes sufficient to suggest stability and repulsion in solution (−11.1 ± 1.8, −18.1 ± 4.3, and −23.1 ± 3.3 mV for Ag A, B, and C, respectively). The observed LSPR λ_{max} for each of the nanoparticles was near the expected value, with the largest diameter nanosphere resulting in the lowest energy LSPR, as indicated by the λ_{max}. The examined Au nanoparticles are in a similar size range, with two different bio-friendly polymeric coatings, either PEG or heparin (HEP). This study examines PEG, for its widespread use to impart stealth character to various materials,[6,7] and HEP, commonly used to impart anticoagulant activity on implanted devices,[22] as two models of material modifications used to modulate potential toxicity. Au PEG nanoparticles were evaluated and found to have an average diameter of 25.6 ± 7.8 nm, while Au HEP had an average diameter of 20.6 ± 15.3 nm. The Au LSPR values for both Au nanoparticles were observed to be similar to literature reports.[16–18] In the case of Au HEP, this suggests the successful preparation of the previously characterized nanoparticles. ζ-potential measurements were performed regularly for up to 48 h following synthesis and purification and suggest that these nanoparticles are stable over the course of the cellular exposures considered herein. In the case of Au PEG, UV-vis spectroscopy was used to assess the transition from seed to PEG-coated nanoparticle: a shift in the LSPR λ_{max} (from 539 ± 1 to 527 ± 4 nm) and a narrowing of the peak half-width (from 96 ± 10 to 69 ± 4 nm) indicates nanoparticle surface modification with PEG that inhibits nanoparticle aggregation (data not shown). The examined Au nanoparticles exhibited negative ζ-potentials of −15.7 ± 3.8 and −42.6 ± 3.3 mV for Au PEG and Au HEP, respectively. Nanoparticles were purified by centrifugation and dialysis (against MilliQ H_2O) prior to characterization and exposure studies. The nanoparticle physicochemical properties were examined by a variety of methods; Table 1 provides a summary of results from these analyses with purified nanoparticles in dye-free media in the presence of 5% serum to model the exposure conditions.

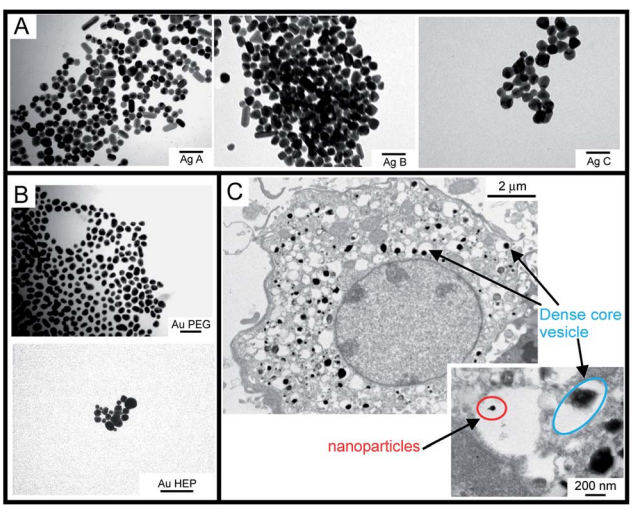

Fig. 1 Transmission electron micrographs of examined nanoparticles and nanoparticle-exposed cells. (A) Ag (B) Au (C) Murine adrenal chromaffin cell after 24 h exposure to Ag C, highlighting the dense core vesicles (at arrows and blue circle) typical of chromaffin cells, with inset showing a close up of an Ag A exposed cell where nanoparticles are localized within a vesicle.

Viability & nanoparticle uptake

A consideration in any toxicity study is whether exposure to a potential toxicant leads to cell death, as significant decreases in viability are a clear sign of toxicity. Here, cellular viability was examined using the MTT assay, where active mitochondria convert a tetrazolium salt into an insoluble formazan crystal, providing a direct correlation between measured absorbance and number of live cells. To examine possible nanoparticle interference with the MTT assay, cell-free control conditions were examined (data not shown) revealing that the nanoparticles do not cause a false positive result nor does any nanoparticle extinction spectrum overlap appreciably with the measured wavelength for MTT assessment. A summary of cellular viability is shown in Fig. 2 (A & C), showing there was no significant change in viability for any of the nanoparticle-exposed cells when compared to the negative control ($p > 0.05$ by ANOVA with Dunnett's post-test).

Despite unaltered viability, nanoparticle exposure can induce changes in cellular function.[12–14] Herein, nanoparticle uptake was evaluated using ICP-AES (uptake) and TEM (localization). The ICP-AES uptake measured amounts of Ag or Au were converted to the average number of nanoparticles based on the average nanoparticle diameter, as described previously.[12,13] As shown in Fig. 2, for Ag nanoparticles there is an inverse size-dependent trend in uptake (all conditions significantly different, $p < 0.05$) with the smallest nanoparticles having the highest number of nanoparticles per cell (average calculated at $1.7 \times 10^5 \pm 3.6 \times 10^4$). In the case of Au PEG, the calculated number of nanoparticles per cell was found to be $2.5 \times 10^5 \pm 4.4 \times 10^4$ on average. For the other Au preparation, Au HEP, the level of uptake was similar to that seen with Au PEG (number per cell was $2.9 \times 10^5 \pm 7.3 \times 10^4$). These results suggest that, despite unaltered viability, cells are, in fact, associating with nanoparticles to a considerable extent. While ICP-AES provides a quantitative measure of nanoparticle association/uptake, it does not prove that the nanoparticles were internalized (though the cells were thoroughly washed prior to acid lysis). To address this issue, localization was evaluated with TEM analysis of sectioned cells after nanoparticle exposure. As with similar, previous studies,[12] nanoparticles were found to be internalized within the cells (Fig. 1C). These results reveal that, despite nanoparticle uptake and localization within cells, the examined nanoparticles do not kill cells.

Carbon-fibre microelectrode amperometry

As reported in previous studies,[12–14,23] even when nanoparticles do not alter cell viability, critical cell functions can be altered. Herein, we examine the possibility of changes in exocytosis function (a mechanism of cellular communication) in MAMCs after 24-hour exposure to the aforementioned series of noble

Table 1 Summary of the physicochemical properties of Ag and Au nanoparticles examined, including three sizes of Ag and two surface-modified Au preparations. The reported physicochemical properties were for purified nanoparticles at 1 nM nanoparticles in dye-free DMEM/F12 media with 5% serum

	Diameter			
Nanoparticle	DLS (nm)	TEM (nm)	ζ-potential (mV)	LSPR (λ_{max}, nm)
Silver				
Ag A	25.8 ± 7.5	18.6 ± 5.1	−11.1 ± 1.8	404.1 ± 4.2
Ag B	44.8 ± 13.1	36.0 ± 6.1	−18.1 ± 4.3	410.9 ± 2.1
Ag C	40.4 ± 11.7	54.5 ± 7.8	−23.1 ± 3.3	431.8 ± 3.5
Gold				
Au HEP	29.7 ± 8.7	20.6 ± 15.3	−42.6 ± 3.3	546.2 ± 2.5
Au PEG	65.2 ± 19.2	25.6 ± 7.8	−15.7 ± 3.8	527.3 ± 3.7

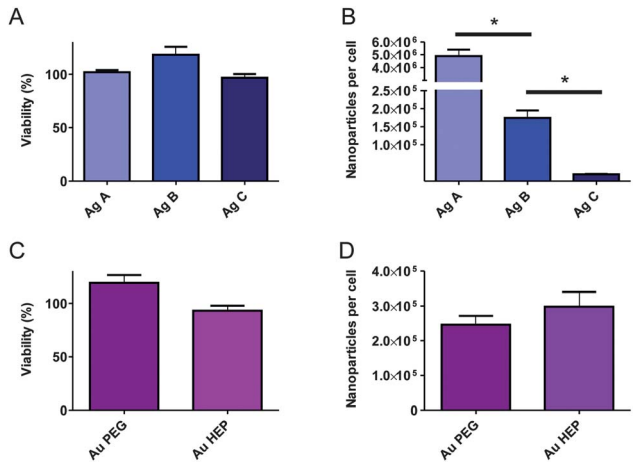

Fig. 2 Summary of viability (as a percent of the negative, unexposed to nanoparticle control cell viability) and uptake (expressed as number of nanoparticles per cell, as calculated from metal concentrations determined by ICP-AES) after 24 h exposure to Ag and Au nanoparticles. (A) Cellular viability was unchanged for all three examined sizes of Ag A at 24 h exposure to 1 nM nanoparticles (B) Ag nanoparticle uptake showed the highest number of nanoparticles per cell, with appreciable uptake for all examined Ag sizes (* denotes $p < 0.05$ by Dunnett's post test after ANOVA) (C) Au-exposed viability was also unchanged, similar to Ag in (A) (D) Au nanoparticle uptake showed similar levels of uptake for both Au PEG and Au HEP.

metal nanoparticles. As a control, MAMCs were exposed to PBS in equal volume to the volume of nanoparticle solution used to ensure that any exocytosis changes were not due to media or buffer dilution effects. Data from different experiments (on at least two separate days) were pooled only when control conditions were not statistically different from each other (t-test, $p > 0.05$). Spike-by-spike analysis was performed for each condition and average spike parameters for each condition were compared (for at least 15 cells using ANOVA, $p < 0.05$). The compiled data was assessed, and data was excluded only when the log mean of a trace was more then two standard deviations outside of the log mean for a given experimental condition. In the case of MAMC exposure to Au HEP nanoparticles, amperometric traces could not be measured, as cells were more fragile than the control cells. Specifically, when being examined during CFMA, a cell would detach from the petri dish surface upon approach by the microelectrode (or stimulating pipette). As this was only found for the Au HEP-exposed conditions, it appears that the examined Au HEP nanoparticles may be interfering with the cellular adhesion process. A separate heparin control, prepared as for the nanoparticle synthesis (concentration), showed similar alterations in cellular adhesion (data not shown). This suggests that free heparin was likely released from the purified nanoparticles and is responsible for the altered adhesion; heparin has been shown previously to modulate adhesion processes in other cell types.[24,25] Future experiments will focus on synthesis of alternate heparin ligands with multiple thiol anchoring groups, though these are not commonly employed in functionalized nanoparticle synthesis.

A key parameter to examine in CFMA studies is the spike area or the charge (Q) due to oxidation of a single granule's epinephrine/norepinephrine content. Any changes in the Q parameter upon nanoparticle exposure reveal the impact of nanoparticles on the chemical messenger loading and/or storage capacity of the vesicles. Here the data shows, in Fig. 3A, that none of examined Ag nanoparticles at the tested concentrations altered the number of moles of epinephrine released from individual chromaffin cells. This was consistent with previous work using CFMA and Ag nanoparticles (61 ± 22 nm), which also found that Q was not decreased at similar dosing and exposure times.[12] In those same experiments, another parameter was found to be perturbed by exposure to nanoparticles - that was the kinetics of vesicular release, reported as $T_{1/2}$. When comparing the nanoparticle-exposed conditions with the PBS control, the

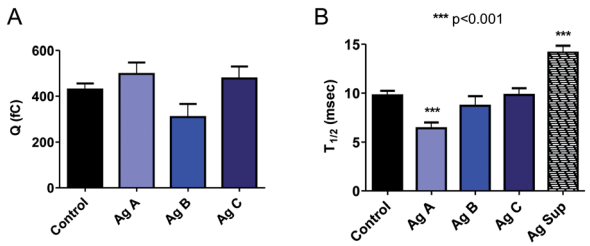

Fig. 3 Summary of carbon-fibre microelectrode amperometry results after 24 h Ag exposure (A) Unaltered spike area (Q), related to the number of the molecules released from vesicles, was seen for any Ag exposure (B) Decreased $T_{1/2}$, indicating a hastening of the kinetics of release, was seen for the smallest examined Ag nanoparticle, opposite the effect seen for the Ag^+ control (Ag Sup, increased $T_{1/2}$) using the Ag A nanoparticle supernatant, accounting for possible nanoparticle dissolution leading to Ag^+ release, suggesting a nanoparticle effect.

smallest Ag (A) was found to induce vesicle content release significantly more quickly than the control condition (6.4 ± 0.6 *versus* 8.9 ± 0.5 ms, $p < 0.005$). For the other examined nanoparticles, the $T_{1/2}$ values were not significantly different from the control condition ($p > 0.05$, Fig. 3B). Given that the calculated average number of nanoparticles per cell was the highest for cells exposed to the smallest (Ag A) nanoparticles, the faster release of epinephrine/norepinephrine could be due to the significantly larger uptake in nanoparticles compared to the other Ag nanoparticle exposure conditions. To investigate the possibility of a Ag dissolution/ion effect,[26] supernatant from the purified nanoparticle was used as an additional control. As shown in Fig. 3B, the supernatant (Au Sup) revealed no effect on Q but did have an effect on the $T_{1/2}$ (increased to 14.3 ± 1.2 ms). This change in the $T_{1/2}$ value in the opposite direction of that measured following Ag nanoparticle exposure suggests that the previously discussed effect on chemical messenger delivery kinetics is, in fact, a nanoparticle rather than an ion effect. Overall, the number of molecules of epinephrine released was unchanged, as represented by Q, though they were expelled more quickly from the vesicle. When this is considered in light of the largest nanoparticle uptake, this suggests that the observed alterations may be due to several possibilities: (1) disruption of the biopolymer matrix unfolding, a major driving force responsible for the kinetics of vesicle release, by the nanoparticle itself, or (2) reorganization of the vesicle composition (fractions of epinephrine, either associating or not associating with the biopolymer matrix) such that there was an increase in the unbound fraction of epinephrine/norepinephrine.

Unlike the changes seen with the smallest examined Ag nanoparticles, surface-modified Au PEG nanoparticles of similar size did not alter the kinetics of release ($p > 0.05$, Fig. 4B). Instead, the Au PEG nanoparticles were found to significantly decrease the number of epinephrine/norepinephrine molecules released after 24-hour exposure ($p < 0.005$, Fig. 4A). This result is similar to that observed in a study with citrate-capped Au nanoparticles (28 ± 4 nm), where Q was seen to decrease after nanoparticle exposure.[12,13] Here, the number of released epinephrine/norepinephrine molecules decreased by 47% ($7.1 \times 10^5 \pm 9.9 \times 10^4$ fewer molecules per vesicle on average). Q provides insights into the vesicular storage of epinephrine/norepinephrine; therefore this disruption reveals a significant alteration to either the loading of the vesicle or the storage capacity of the vesicle after exposure to Au PEG. When compared to previous work,[12] this decrease in Q suggests that the addition of a PEG coating did not completely alleviate the previously described disruption to exocytosis (altered Q and $T_{1/2}$ values) as one might expect given the stealth character often imparted by a PEG coating. Overall, these results suggest that a more complex mechanism than simple surface interactions between the nanoparticle and matrix affect exocytosis disruption. While the examined PEG surface modification to Au lead to a reduction in the perturbation to the kinetics of release it did not alter the number of molecules released, suggesting that a surface effect may be involved in the $T_{1/2}$ but not the Q parameters. In the case of $T_{1/2}$, a major driving force within the vesicle is the matrix unfolding upon fusion with the plasma membrane.[27,28] If a nanoparticle were interacting directly with the vesicle matrix, the kinetics of release would be modulated and alter the $T_{1/2}$ value accordingly; abrogation of the nanoparticle-vesicle matrix interaction would therefore relieve the disruption and restore normal kinetics. The observed alteration in the Q values for exocytosis release could be explained by a volume change within the vesicle due to the nanoparticle uptake within the vesicle itself. Given that the concentration of epinephrine is known to be constant across vesicles,[29] the presence of nanoparticles within the vesicle may alter the maximum storage capacity (total number of molecules stored) by altering the 'available' volume within the vesicle (as increased nanoparticle volume leads to corresponding decreases in the epinephrine-containing volume in the vesicle). In the case of the addition of PEG to the Au surface, nanoparticle exposure would alter the available vesicle volume, as it did for Au without PEG, and would continue to alter the Q parameter (as described) but would alleviate the previously suggested nanoparticle-biopolymer matrix disruption[12–14] which would restore the kinetics of release as seen for the reported $T_{1/2}$ value.

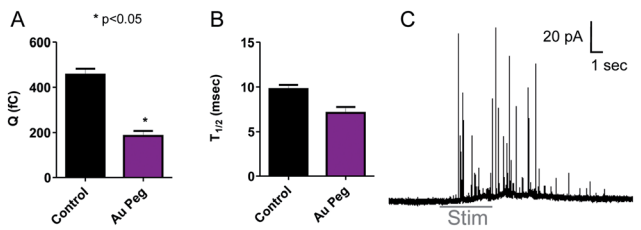

Fig. 4 Summary of carbon-fibre microelectrode amperometry results after 24 h Au PEG exposure (A) A decrease in spike area (Q, * denotes $p < 0.05$ by ANOVA with Dunnett's post test) was seen, indicating fewer molecules were released from the vesicles while (B) the kinetics of release remained the same. (C) A carbon-fibre microelectrode amperometry trace from Au PEG-exposed cell where the bar indicates the period of cell stimulation with 60 mM K^+ (Stim).

Conclusions

Due to the differences in study approaches, including varied model cells, nanoparticles, and toxicity assessments, there is currently a lack of consensus regarding the key physicochemical properties and mechanisms involved in nanoparticle toxicity. The work described herein addresses this paucity of data by further examining noble metal nanoparticle exposure in chromaffin cells. To summarize, this work examines the effect of size on Ag nanoparticle alterations of exocytosis function after 24 h exposure in murine chromaffin cells. Using Ag nanoparticles, with an average diameter between 15 and 60 nm, cells exhibited unaltered viability after inversely proportional size-dependent uptake. This uptake correlated with a significant increase in the speed of the release kinetics as measured by CFMA. Nanoparticle supernatant induced a slowing of the release kinetics, suggesting a nanoparticle-specific change rather than an ion release effect. Examinations of the effects of PEG-coated Au also demonstrated unaltered cellular viability, despite nanoparticle uptake. These Au PEG nanoparticles altered exocytosis release by decreasing the number of molecules of epinephrine/norepinephrine released from each vesicle, but the surface PEG modification restored previously described alterations to the kinetics of release (after citrated Au exposure), further supporting the

previously proposed[12–14] nanoparticle-vesicle matrix disruption. In the case of heparin-coated Au, while cells take up nanoparticles and do not show decreased viability after 24-hour exposure, cellular adhesion was altered to the point where CFMA examinations were not possible, likely due to the release of free heparin from the nanoparticles. The results found here further support the body of work revealing that noble metal nanoparticles do perturb the process of exocytosis, typically altering the number of molecules and kinetics of release from vesicles. Overall, these results suggest that various physicochemical properties including size and surface coating do modulate changes in cellular communication *via* exocytosis as measured with CFMA.

Acknowledgements

Financial support of this work was generously provided by the National Science Foundation (No. CHE-0645041).

Notes and references

1 Woodrow Wilson International Center for Scholars, Project on Emerging Nanotechnologies: Inventory of Nanotechnology Consumer Products. nanotechproject.org.
2 A. Alkilany and C. Murphy, *J. Nanopart. Res.*, 2010, **12**, 2313.
3 D. Walczyk, F. Bombelli, M. Monopoli, I. Lynch and K. Dawson, *J. Am. Chem. Soc.*, 2010, **132**, 5761.
4 M. Safi, J. Courtois, M. Seigneuret, H. Conjeaud and J.-F. Berret, *Biomaterials*, 2011, **32**, 9353.
5 M. Lundqvist, J. Stigler, G. Elia, I. Lynch, T. Cedervall and K. Dawson, *Proc. Natl. Acad. Sci. U. S. A.*, 2008, **105**, 14265.
6 A. Karakoti, S. Das, S. Thevuthasan and S. Seal, *Angew. Chem., Int. Ed.*, 2011, **50**, 1980.
7 M. Joralemon, S. McRae and T. Emrick, *Chem. Commun.*, 2010, **46**, 1377.
8 M. Tarantola, A. Pietuch, D. Schneider, J. Rother, E. Sunnick, C. Rosman, S. Pierrat, C. Sönnichsen, J. Wegener and A. Janshoff, *Nanotoxicology*, 2011, **5**, 254.
9 M. Abdelhalim and B. Jarrar, *Lipids Health Dis.*, 2011, **10**, 133.
10 C. Zanette, M. Pelin, M. Crosera, G. Adami, M. Bovenzi, F. Larese and C. Florio, *Toxicol. in Vitro*, 2011, **25**, 1053.
11 R. Foldbjerg, D. Dang and H. Autrup, *Arch. Toxicol.*, 2010, **85**, 743.
12 S. Love and C. Haynes, *Anal. Bioanal. Chem.*, 2010, **398**, 677.
13 B. Marquis, M. Maurer-Jones, K. Braun and C. Haynes, *Analyst*, 2009, **134**, 2293.
14 B. Marquis, Z. Liu, K. Braun and C. Haynes, *Analyst*, 2011, **136**, 3478.
15 O. Ivanova and F. Zamborini, *J. Am. Chem. Soc.*, 2010, **132**, 70.
16 Y. Liu, M. Shipton, J. Ryan, E. Kaufman, S. Franzen and D. Feldheim, *Anal. Chem.*, 2007, **79**, 2221.
17 T. Niidome, M. Yamagata, Y. Okamoto, Y. Akiyama, H. Takahashi, T. Kawano, Y. Katayama and Y. Niidome, *J. Controlled Release*, 2006, **114**, 343.
18 Y. Guo and H. Yan, *J. Carbohydr. Chem.*, 2008, **27**, 309.
19 R. Borges, J. Diaz-Vera, N. Dominguez, M. Arnau and J. Machado, *J. Neurochem.*, 2010, **114**, 335.
20 K. Kawagoe, J. Zimmerman and R. Wightman, *J. Neurosci.*, 1993, **48**, 225.
21 B. Chithrani, A. Ghazani and C. Chan, *Nano Lett.*, 2006, **6**, 662.
22 C. Werner, M. Maitz and C. Sperling, *J. Mater. Chem.*, 2007, **17**, 3376.
23 B. Marquis, A. McFarland, K. Braun and C. Haynes, *Anal. Chem.*, 2008, **80**, 3431.
24 R. Nelson, O. Cecconi, W. Roberts, A. Aruffo, R. Linhardt and M. Bevilacqua, *Blood*, 1993, **82**, 3253.
25 K. Peter, M. Schwarz, C. Conradt, T. Nordt, M. Moser, W. Kübler and C. Bode, *Circulation*, 1999, **100**, 1533.
26 W. Zhang, Y. Yao, N. Sullivan and Y. Chen, *Environ. Sci. Technol.*, 2011, **45**, 4422.
27 C. Amatore, Y. Bouret, E. Travis and R. Wightman, *Biochimie*, 2000, **82**, 481.
28 C. Amatore, S. Arbault, M. Guille and F. Lemaître, *Chem. Rev.*, 2008, **108**, 2585.
29 R. Wightman, J. Jankowski, R. Kennedy, K. Kawagoe, T. Schroeder, D. Leszczyszyn, J. Near, E. Diliberto and O. Viveros, *Proc. Natl. Acad. Sci. U. S. A.*, 1991, **88**, 10754.

